International Journal of Thermodynamics (IJoT)
ISSN 1301-9724 / e-ISSN 2146-1511
https://dergipark.org.tr/en/pub/ijot

Vol. 27 (No. 2), pp. 027-036, 2024
doi: 10.5541/ijot.1330933
Published online: June 1, 2024

Research Article

Analytical Modeling of Counter-Current Drying Process

*M.T. Pamuk

Okan University, İstanbul, Turkey
E-mail: *turgaypamuk@hotmail.com

Received 21 July 2023, Revised 19 September 2023, Accepted 07 February 2024

Abstract

In this analytical study, spray drying of detergent particles of diameters 0.4-1 mm by using counter-current air heated at around 300°C is investigated using Matlab©. Particle drying using hot gases is a mature process with a vast variety of applications ranging from dried food to powdered detergent production. The study shows a strong relationship between the drying process (final water content) and particle size, drying gas temperature, as well as the tower dimensions since cross-sectional area of the tower has a direct control on vertical gas velocity, thus heat and mass transfer coefficients while the height of tower is closely related to residence time of particles in tower which guarantees the targeted drying level. The conclusions of this study can be a guide to have a better set of drying parameters such as inlet temperatures and humidity/water content as well as exit temperatures and humidity/water content and valuable information on how these relate to heat energy consumption necessary to heat the air from atmospheric conditions to the desired drying gas temperature. It is also worth indicating that the measurement of the absolute humidity in tower exhaust is a good parameter to control the drying process in an effective way.

Keywords: *Heat transfer; convection; mass transfer; spray drying; counter-current dryers.*

1. Introduction

Particle drying is a complex phenomenon involving coupled heat and mass transfer as well as particle kinematics caused by vigorous mixing in a drying tower. Heat transfer occurs mainly in convection mode while mass transfer is an outcome of water vapor migration due to evaporation of water caused by concentration difference between the water content on the surface of the particle and the drying medium. As the drying takes place at the surface of the particle, there also occurs a mass transfer of water from the internal part of the particles to its surface due to the concentration gradient. This process continues until the particle dries to the targeted water content. Research in the area is vast ranging from analytical studies to experiments as well as numerical simulations. Mujumdar and Jog [1] proposed a simple procedure for the design of a spray drying tower especially suitable for drying of skim milk where drying gas temperature is at the vicinity of 200°C and the powder dimension is about 100μm. Despite the simplicity of the design process and the assumptions, they point out that their model can accurately predict the required tower and nozzle dimensions as well as power requirements. The model studied in this paper is checked with their data for comparison. However, some deviations are found mainly because their tower has concurrent flow as opposed to counter-current studied herein. Wawrzyniak et al. [2] presented in their paper both theoretical and experimental determination of hydrodynamics of drying air in the industrial counter-current spray dryer. They compared experimental and theoretical results and showed that the developed CFD model of counter current spray drying process can be used for a reliable estimation of the tower performance. Ali [3] investigated the simple plug-flow model in a pilot counter-current spray drying tower in his PhD thesis by comparing the results of numerical simulations to those of experiments performed by previous researches. According to his findings; the simple plug-flow model has the advantage of being cheap in computational resources and can be used to determine the influence of various operating parameters. Afolabi and Onifade [4] developed a fundamental model that can be used to predict the air residence time distribution of spray droplets in a counter-current spray dryer. Their simulation results show that most of spray evaporation is completed within a short-time interval meaning that the mean size of the pure liquid spray increases with time due to the rapid completion of evaporation of the smaller droplet sizes in the spray. They also indicate that there is a close agreement between the simulated result and experimental data. Ali et al. [5] implemented a steady state, three-dimensional, multiphase CFD simulation of a pilot-plant counter-current spray drying tower with an emphasis put on the modeling of particle-wall interaction. They found that the particle-wall interaction was one of the critical factors influencing the predicted average dried powder characteristics. Crosby et al. [6] investigated the effects of particle size on drying performance. They concluded that cascade control of the mean particle size, based on manipulating the mass flow rate of gas, resulted in tighter, more responsive control. They also indicate that changes in slurry rate caused complications, as the impact on particle size growth in the dryer is non-linear and difficult to predict. Gonzalez-Gallego et al. [7] investigated a co-current flow spray drying tower for maltodextrin drying using an analytical and numerical model in their study. They indicate

*Corresponding Author

that their proposed model differs from a classic counter-flow model as it can predict dynamic changes even with a dispersed phase with variable velocity and it is able to predict composition, temperature and velocity of both phases, continuous and disperse, at axial points in the tower. Hernandez et al. [8] presented a novel CFD model in which different levels of deposition and Reynolds numbers for swirling-flow industrial-scale spray-drying towers are taken into account. They initially compared steady-state and transient simulations, then calibrated their CFD model using the experimental swirl intensity values under different levels of deposits. The methodology is only applicable to steady-state solutions, since the dynamic equilibrium between deposition and re-entrainment is achieved and the deposits are constant, in terms of time. They point out that it does not consider the simultaneous interaction between the deposits generated and the effect that they create on the flow. Xia et al. [9] investigated the heat and mass transfer performances of the spray drying tower under different pressures in order to explore the optimum pressure in the drying tower. They developed a three-stage heat and mass transfer model for single-droplet in their simulation to show the effect of pressure on tower height and inlet air temperature required for droplet to be completely dried. They found that the optimal pressure is increased with the increase of inlet air temperature. However, when the tower height is fixed, the inlet air temperature required for drying droplet firstly decreases and then increases with the increase of pressure. They also indicate that it is feasible to achieve complete drying in spray drying process by reducing the pressure in the tower with low inlet temperature. Jamil Ur Rahman et al [10] presented in their research an experimental analysis of a counter flow spray drying process using water and skim milk as feed. They performed their study by examining the droplet size distribution of sprays and the temperature profiles in the dryer. They evaluated the influence of air inlet temperature, air mass flow rate, feed flow rate, and droplet size on air temperatures in the dryer. Their results show that it is possible to have a process intensified spray drying technology in a counter-current setup using an elevated air temperature of 260–360ºC. They point out the main problem for the high-temperature milk spray drying in a small volume is the accommodation and control of various size droplets with different velocities and drying rates, and the separation of such droplets/particles before they impinge the walls. However, the introduction of swirling flows at these locations should reduce the problem. Sefidan et al. [11] investigated in their study the spray drying process of whole milk by providing statistics on droplet conditions at exit and first impact with the surfaces of the chamber using a numerical model. They validated a four-stage droplet evaporation model against an experiment and then coupled to an Euler–Lagrange model for simulating the milk droplet trajectories inside a dryer. Their results show that larger droplets remain for a shorter residence time in the tower and contain more moisture on exiting. According to their findings regarding the drying conditions, the residence time is not affected by a decrease in the airflow inlet temperature from 200°C to 150°C. However, since the evaporation rate decreased, the result was more droplets leaving the dryer with a higher moisture content. Jubaer et al [12] assessed in their work, five different turbulence models in CFD simulations of a lab scale counter-current spray drying process. They concluded that the tested turbulence models with default settings are unlikely to provide a good agreement between the simulation and measured data, particularly for a lab scale dryer, where the flow field might not be entirely turbulent, despite the available low Reynold number corrections. They also point out that their work will prove extremely useful in simulating spray drying applications in a lab scale as well as industrial spray dryers, since the choice of an appropriate turbulence model can considerably improve the accuracy of the prediction. Hernandez et al. [13] evaluated in their study the single droplet drying (SDD) of detergents. They used experimental data are to validate a theoretical multistage model. According to their findings, drying appears to take place in three stages: The first stage being a surface drying stage with a shrinkage of the droplet until the surface gets saturated, the second stage where the drying is governed by the diffusive resistance of water through the pores and the third stage controlled by boiling temperature until the final equilibrium moisture content is achieved. Chen et al. [14] proposed a one-dimensional mathematical model for the drying process of calcium chloride solution in a co-current spray separation tower based on the four-stage drying model of single droplet. Their simulation results show that air mass flow rate, inlet solution concentration and solution mass flow rate have a greater effect on the thermal efficiency than other inlet parameters while the inlet solution concentration plays a pivotal role on the drying strength. According to their conclusions, the air mass flow rate, inlet solution concentration and solution mass flow rate have greater effect on the thermal efficiency than other parameters. Also, there exists an optimal dry air mass flow rate at which the drying strength and volumetric heat transfer coefficient are the maximum values, while the dry air mass flow rate has negative effect on the thermal efficiency, and the most significant impact on the volumetric heat transfer coefficient is the inlet solution concentration heat transfer coefficient.

In this study, the physical and process data of an example tower are considered for the analysis of the drying performance of a counter-current spray dryer. It is believed such an analytical study presented herein can make it possible to fine tune the tower to optimum operating conditions especially towards the energy efficiency of the drying tower.

2. Analytical Model

In spray drying of particles such as powdered detergent, high water content (typically 20-40%) material is forced through nozzles of small diameters at high pressure by means of special pumps into a drying tower (Figures 1 and 2). The numerical values on both figures are either directly excerpted from production data of Ali [4] or estimated/calculated by using his data. The wet particle in a drying tower meet air at average temperatures well over 200ºC flowing in the opposite direction, usually in a swirling motion to enhance the heat and mass transfer and to help increase the residence time of the particle in the tower.

Particle kinematics plays an important role in spray drying. Newton's second law states that the sum of all external forces on a body must be equal to a dynamic force which is the product of mass and acceleration. While the initial vertical velocity of the particles leaving the nozzles are quite high (typically at an order of 50-100 m/s), they tend to decelerate to much lower velocities in a short time due to drag forces between the particles and gas in opposite flow as well as a net force between the gravitational and buoyancy forces. As a result of deceleration, particles slow down a

velocity of less than 10 m/s. Particles' residence time is then determined by this deceleration as well as the increased path length due to the swirling motion of the hot drying air supplied from specially directed gas inlets at the cone section of the bottom of the tower.

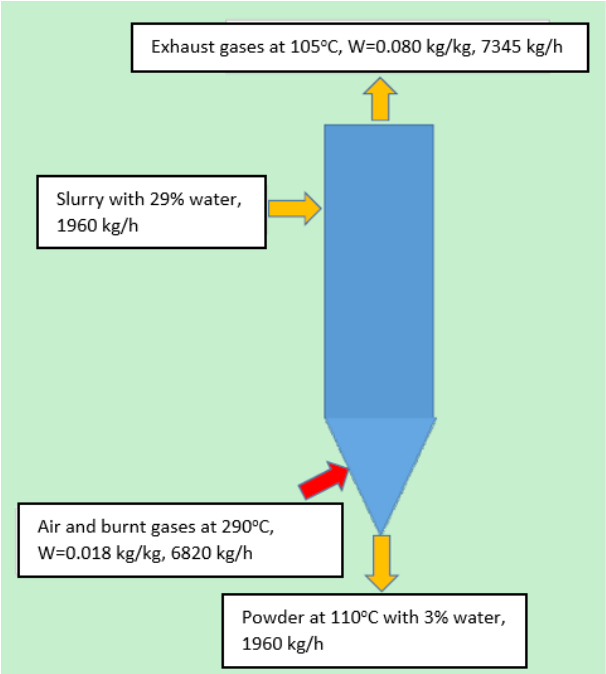

Figure 1. Counter-current drying tower (Mass balance). (Figure is in color in online version of paper).

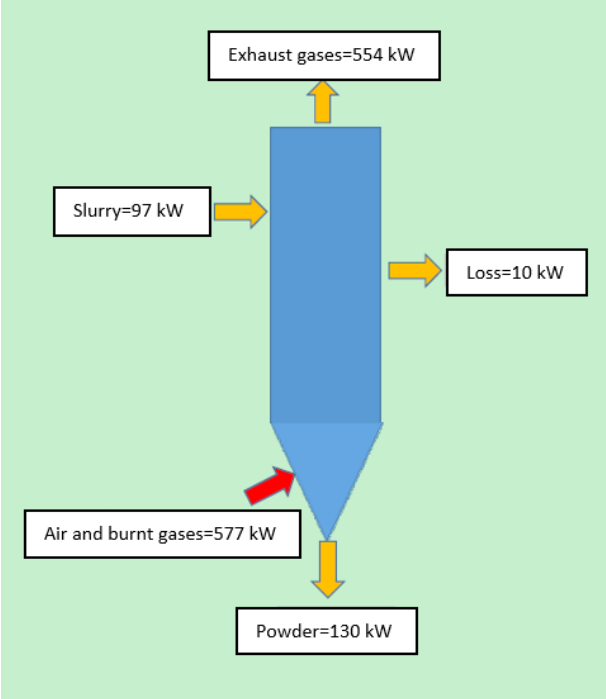

Figure 2. Counter-current drying tower (Heat balance). (Figure is in color in online version of paper).

It should be noted that the swirling strength determining the residence time is an effective vortex indicator in wall turbulence, and it can be determined based on three-dimensional (3D) velocity fields. In this context, drying throughput of the tower is strongly related to its volume which is calculated by the tower diameter and height. The smaller the diameter, the higher the vorticity, thus a larger tower height and a longer residence time. Preliminary design of a drying tower requires an extensive study of particle kinematics. Figure 3 shows the velocity streamlines for fluid phase in a counter-current drying tower (from an unpublished work of the author).

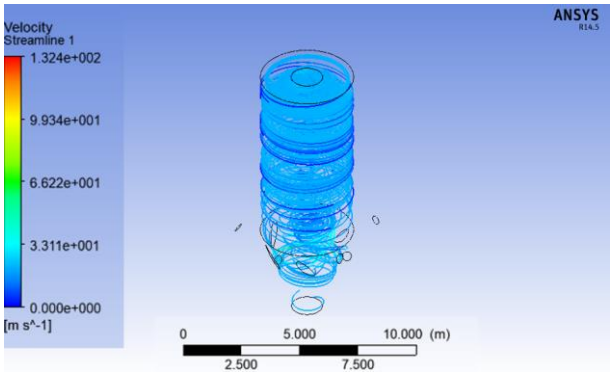

Figure 3. Velocity streamlines. (Figure is in color in online version of paper).

Once the dimensions of the tower determined using kinematic principles, methods of heat and mass transfer are implemented as drying is a result of these two principles. On one hand, convection occurs between the particle and the drying medium which is most of the time a mixture of air and hot gases as given in Equation 1 [15]:

$$\dot{Q}_{conv} = hA_o\,(T_o - T_\infty) \tag{1}$$

where h is convection coefficient which is dependent on many factors such as geometry and surface characteristics of the particle, flow and/or particle velocity and fluid properties. T_o and T_∞ are particle surface and fluid temperatures, respectively. On the other hand, water content of the particle is reduced due to the evaporation caused by concentration gradients and differences as given in Equations 2 and 3 respectively, as given by Çengel [15]:

$$\dot{m}_{diff} = -D_{AB}A\frac{dC}{dx} \tag{2}$$

$$\dot{m}_{conv} = h_{mass}\,A_o\,(\rho_o - \rho_\infty) \tag{3}$$

where h_{mass} is convective mass transfer coefficient and ρ is water vapor density with the subscripts o (outer surface) and ∞ (far field). Equation 2 is Fick's law which is analogous to Fourier's law in that they both are diffusion phenomena where the diffusion coefficients and variation of properties through the thickness of material (variation per unit length of the material or gradient) are the driving effects. Fourier's law gives conduction heat transfer (*e.g. kJ/s*) while Fick's law gives mass transfer (*e.g. kg/s*) depending on the diffusion coefficient (mass diffusivity) D_{AB} and concentration gradient dC/dx. A is the area perpendicular to flow in both equations. Equation 3 is analogous to Equation 1 in that they both utilize convective coefficients and differences of temperatures and concentrations. A_o is the surface area of the particle in both equations. If particle is assumed to be a sphere, Equation 2 is valid for the drying phenomenon taking place within the particle due to the water concentration variation through the radius of the particle (concentration gradient) while Equation 3 is valid for the evaporation phenomenon from the surface of the particle and the fluid due to the water concentration difference between the particle surface and the fluid. D_{AB} is strongly related to physicochemical properties of the particle

material and usually readily available while h_{mass} is much more complicated to determine.

Particles lose most of their water content according to Equations 2 and 3 as they travel from the nozzle from where they are sprayed towards the bottom of the tower under the influences of the net vertical force (gravitational and buoyancy) and drag force caused by the upward swirling air. If these two equations are set equal to each other, it is interesting to point out the analogy between lumped heat transfer and lumped mass transfer in which it is possible to describe a parameter similar to Biot number in transient heat transfer. Parti [16] performed an analytical study regarding the similarity between mass transfer Biot number and heat transfer Biot number and concluded that all the results and statements on heat transfer are applicable for mass transfer substituting the heat transfer Biot number by mass transfer Biot number.

The heat and mass transfer for the particles within the tower is a transient process as neither humidity nor the temperature of the particle remains constant throughout the process, although the particle temperature variation is much less compared to water content variation. The evaporation process causing a reduction in particle's mass and convective heat transfer causing a change in particle's temperature with the inclusion of particle's internal energy variation due to the time dependent nature of physical phenomenon can be simplified by introducing the following mathematical model (Equation 4) which belongs to the coupled heat and mass transfer [7]:

$$L\frac{dm}{dt} + hA_o\,(T_o - T_\infty) = mc\frac{dT}{dt} \tag{4}$$

where L is latent heat of water, or in other words energy required for the water phase to change to gas phase during the evaporation and m and c are the mass and the specific heat of the particle, respectively. Particle temperature may remain almost constant for most of the process due to the thermal balance between the evaporative cooling and convective heat gain, although their temperature tends to increase fast as their water content become very low towards the end of the process.

Initial gas temperature T_∞ can be calculated by considering the adiabatic flame temperature of the combustion products of natural gas (*mostly methane*, CH_4) as given in Equation 5 [17]:

$$CH_4+2O_2+2(3.76)N_2 \rightarrow CO_2+2H_2O+2(3.76)N_2 \tag{5}$$

where *891 kJ/mol* energy is released. The coefficient 3.76 comes from the molar ratio of N_2 to O_2 in the atmospheric air. Above equation belongs to stoichiometric combustion of methane where the stoichiometric air/fuel ratio is $AF_{sto}=m_{air}/m_{methane}=274.6/16=17.2$. It should be noted that the chemical energy of combustion is less than *891 kJ/mol* (*HHV*) due to the fact that product water is vapor, not liquid, thus it absorbs latent heat required for vaporization. If the heat of vaporization of water is taken to be $i_{fg}=2260$ *kJ/kg=40.7 kJ/mol*, then for 2 *mols* of product water to evaporate, the stoichiometric combustion requires *2x40.7=81.4 kJ* per mol of natural gas. Therefore, net heat energy released during the chemical reaction is taken to be *891-81.4~809 kJ/mol (LHV).*

Two different analyses are performed within this study:

1. Overall mass and heat balance to and from the drying tower
2. Heat and mass interaction of individual particles as they travel within the tower

In all drying processes, the target is a predefined water content of the final product (w_p). Mass flow rate of wet product, or slurry ($\dot{m}_s$) is measured using a mass flow meter before it is supplied to tower. The process requires that either water content of slurry (w_s) or mass flow rate of dry product ($\dot{m}_p$) be known. Assuming w_s is known, following relation between $\dot{m}_s$ and $\dot{m}_p$ is obtained from Equation 6:

$$\dot{m}_p = \dot{m}_s(1 - w_s)/(1 - w_p) \tag{6}$$

For the first part of the first analysis, Figures 1 and 2 need to be taken into account for mass and energy balances:

$$\dot{m}_s + \dot{m}_{gas} = \dot{m}_p + \dot{m}_{exh} \tag{7}$$

$$\dot{m}_s i_s + \dot{m}_{gas} i_{gas} = \dot{m}_p i_p + \dot{m}_{exh}\, i_{exh} + \dot{Q}_{loss} \tag{8}$$

where $\dot{Q}_{loss}$ is the heat lost to the surroundings from the external surface of the drying tower which may be as high as *20%* of the heat input, depending on the overall thermal resistance at tower's wall including its thermal insulation and the temperature difference between the average gas temperature in the tower and ambient temperature as well as cold air entrained at the dry product (powder) exit at the bottom due to the vacuum (in the order of *250 Pa*) at the tower top created by the suction at the exhaust side. Considering this heat loss, assuming the burner combustion efficiency and energy carried away by exhaust gases and dry product, an overall drying process thermal efficiency of η_{dry} *~50%* can be taken into account for initial calculations. However, this needs to be verified by implementing Equation 8. Enthalpies in Equation 8 can be calculated from C_pT for wet and dry products as well as gas while for exhaust gas from Equation 9 as given by McQuiston et al. [18]:

$$i_{exh} = T_{exh} + W_{exh}(2501.3 + 1.86T_{exh}) \tag{9}$$

where i is the specific enthalpy.

Using ideal gas law $\rho=P/(RT)$, density of natural gas is calculated, then the mass flow rate of natural gas can be obtained as $\dot{m}_{CH_4}=\rho\dot{V}_{CH_4}$ where $\dot{V}_{CH_4}$ is the volumetric flowrate of natural gas.

By revisiting Equation 5, the adiabatic flame temperature of the stoichiometric combustion can be calculated using Equation 10 and 11 as given by Pulkrabek [17].

$$\dot{m}_{CH_4} + \dot{m}_{air} = \dot{m}_{CO_2} + \dot{m}_{H_2O} + \dot{m}_{N_2} = \dot{m}_{sto} \tag{10}$$

$$\dot{m}_{CO_2}C_{p,CO_2}\Delta T_{adia} + \dot{m}_{H_2O}C_{p,H_2O}\Delta T_{adia} + \dot{m}_{N_2}C_{p,N_2}\Delta T_{adia} = \dot{m}_{CH_4}(LHV) \tag{11}$$

Constant temperature specific heats seen in Equation 11 are usually temperature dependent especially at temperatures such as found in flames. Using constant pressure specific heat values for C_{p,CO_2}, C_{p,H_2O} and C_{p,N_2} as *48.2 kJ/mol.K*, *31.6 kJ/mol.K* and *29.4 kJ/mol.K* respectively, the

calculation yields an adiabatic temperature of about T_{adia}=2350°C. It is therefore possible to calculate the mass flow rate of ambient (excess) air $\dot{m}_{exc}$ as given in Equation 12 and 13:

$$\dot{m}_{gas} i_{gas} = \dot{m}_{sto} C_p T_{adia} + \dot{m}_{exc} i_{exc} \quad (12)$$

$$\dot{m}_{gas} = \dot{m}_{sto} + \dot{m}_{exc} \quad (13)$$

and the air enthalpies can be calculated as in Equation 12 and C_p=32.4 kJ/mol.K, a weighted average of C_{p,CO_2}, C_{p,H_2O} and C_{p,N_2}. Once $\dot{m}_{exc}$ is known, all the mass flowrates can be calculated.

The humidity content of the above drying gas is very small when considered as relative humidity at the given temperature and its adverse effect on drying is negligible. However, as the evaporation from particles takes place, the water vapor content (humidity) in gas flowing towards the exit increases substantially as can be seen from Equations 14 and 15, as evaporated water will be added in gas flow.

$$\dot{m}_w = \dot{m}_{wet} - \dot{m}_{dry} \quad (14)$$

$$\dot{m}_{exh} = \dot{m}_{gas} + \dot{m}_w \quad (15)$$

For the second analysis, Matlab© is used for the calculation of the overall heat and mass transfer between the particle and the gas. Equation 4 can be solved iteratively by taking the final humidity target to terminate the calculation. The most critical part of this equation is the dying rate, or *dm/dt* that must be calculated by considering Equation 2. A better presentation of this equation is given in Equation 16 which is given for a hollow spherical particle:

$$\dot{m}_{diff} = 4\pi r_1 r_2 D_{AB} \frac{\rho_1 - \rho_2}{r_2 - r_1} \quad (16)$$

Internal surface of the hollow cylinder can be taken to be saturated at the given particle temperature which makes it possible to determine ρ_1. However, the surface water content ρ_2 is not readily available. On the other hand, at the particle-gas interface mass flow rates due to diffusion and convection must be equal, i.e. $\dot{m}_{diff} = \dot{m}_{conv}$. This equality makes it possible to eliminate ρ_2 in Equations 3 and 16, however h_{mass} is still an unknown, but it can be calculated using Chilton-Colburn analogy:

$$\frac{h_{heat}}{h_{mass}} = \rho C_p \left(\frac{\alpha}{D_{AB}}\right)^{2/3} \quad (17)$$

where α is the thermal diffusivity, D_{AB} is the diffusion coefficient of vapor in the air (different from D_{AB} in the particle which is the diffusion coefficient of water in the particle) and can be calculated from Equation 18:

$$D_{AB} = 1.87x10^{-10} \frac{T^{2.072}}{P} \quad (18)$$

h_{heat} is calculated from Nusselt number ($Nu=hd/k$) for flow about spherical surfaces as proposed by Whitaker [19]

$$Nu = 2 + \left(0.4Re^{1/2} + 0.06Re^{2/3}\right) Pr^{0.4} \left(\frac{\mu}{\mu_s}\right) \quad (19)$$

which is valid for $0.71 \leq Pr \leq 380$,

$$3.5 \leq Re \leq 7.6x10^4 \text{ and } 1.0 \leq \left(\frac{\mu}{\mu_s}\right) \leq 3.2$$

Above equations are evaluated sequentially and iteratively once the required reduction in water content of the final product calculated, as well as the corresponding energy requirement. The iterative calculation scheme (flowchart) is given in Figure 4.

3. Results and Discussion

For simulation purposes, standard atmospheric pressure and temperature (P_a =101.3 kPa and T_a = 20°C) with a relative humidity of RH_a = 50% (W_a=0.0072 kg of water per kg of dry air) are assumed. In order to have realistic simulation results, following production data of Ali [3] is used. Due to the confidentiality requirements set forth by author's institution, some of the following data have been deducted and may not reflect the actual data. For instance, tower area is calculated by using mass fluxes ($kg/m^2.s$) and enthalpy flow rates provided, using the relationships $m''=\dot{m}/A$ and $\dot{Q}_{gas} = \dot{m} i_{gas}$. Once the cross sectional area of the tower is determined, its height is calculated by using the scale of tower drawing.

Input data and stoichiometry calculations:

D = 1.65 m (estimated tower diameter)
H = 16.5 m (estimated tower height)
C_s = 2100 J/kg.C (Data, slurry specific heat)
C_p = 1500 J/kg.C (Data, powder specific heat)
ρ_s = 1200 kg/m³ (Data, slurry density)
$\dot{m}_s$ = 1960 kg/h (Data, estimated)
w_s = 29% (Data)
w_p = 3% (final water content, typical range 2-3%)
$\dot{m}_p$ = 1435 kg/h (Equation 6)
T_s = 85°C (Data)
T_{gas} = 290°C (Data)
T_{exh} =105°C (Data)
d =750μm (assumed, average particle diameter)

Analyses:

As is shown in Figure 1, overall mass and heat balance to and from the drying tower: Mass balance can be obtained from Equation 7:

1960 + 6820 = 1435 + 7345 (checks)

Similarly, as is shown in Figure 2, heat balance can be obtained from Equation 20

$$\dot{m}_s i_s + \dot{m}_{gas} i_{gas} \rightarrow \dot{m}_p i_p + \dot{m}_{exh} i_{exh} + \dot{Q}_{loss} \quad (20)$$

$$97 + 577 = 130 + 534 + \dot{Q}_{loss}$$

It then turns out that $\dot{Q}_{loss}$=10 kW (~1.8% of the energy input which includes the effect of air entrainment also). Drying towers must be insulated against heat loss through the outer tower walls. The loss percentage is therefore a matter of insulation level, thus the loss of 20% represents a very poorly insulated tower. Using the tower data from the published work, we can deduce that the heat insulation of the tower used in this study is good. Particle flow rate:

$\dot{n}_p = \dot{m}_s / m_p = \dot{m}_s / [\rho_s (4\pi r^3/3)] = 2.05x10^6$ particles/s.

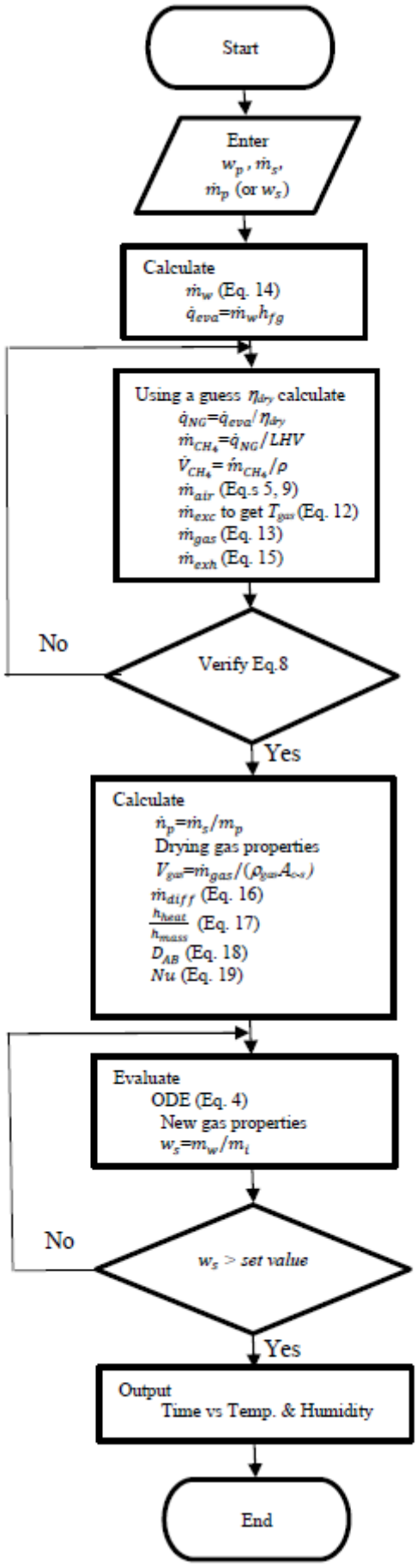

Figure 4. Flowchart of the iterative calculation scheme.

From this point on, the iterative process mentioned above is performed and following simulation results are obtained:

Figure 5 gives the temperature variation of particle and drying air for an average particle diameter of *750 μm*. The drying gas temperature is shown to be at the same instant of particle's dying process time, i.e., gas temperature at *t=0* is the gas exit temperature, not the inlet temperature. When targeted w_s is reached, the iterative calculation is terminated, therefore plot for *t > 5.3* s is not shown.

Drying time and the particle temperature at the exit strongly depends on particle diameter. To illustrate this dependence, it is interesting to investigate Figures 6 and 7. In Figure 6, the particle diameter is 400 *μm* while Figure 7 belongs to a particle with a diameter of 1000 *μm*. Same reasoning for *d*=750 *μm* for terminating the iterative calculation applies also to these cases. It is important to note that the temperature of the particle drops drastically at the beginning of the drying process due to the evaporative cooling caused by very high rate of mass transfer from the particle to its surroundings. As the drying proceeds, convective heat transfer becomes more accentuated where heat flows from the gas to particle causing its temperature to increase. It is vital to have a control on the exit humidity and the temperature of the particle, thus its size as well as drying gas properties are very important. This effect is seen in Figure 8 where $f=\dot{Q}_{evap}/\dot{Q}_{conv}$.

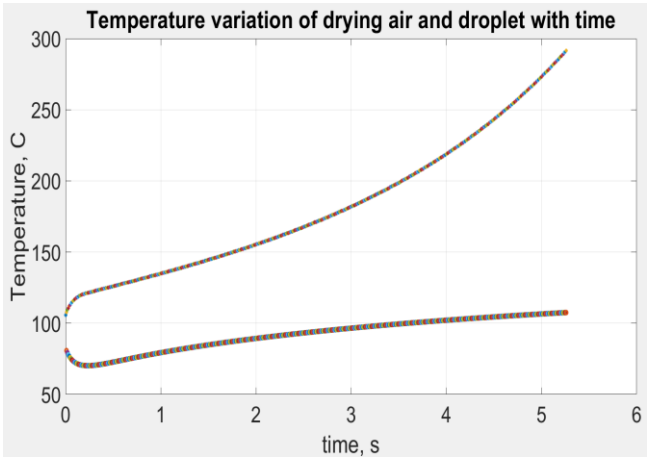

Figure 5. Temperature variation of drying air (top) and particle (d=750 μm). (Figure is in color in online version of paper).

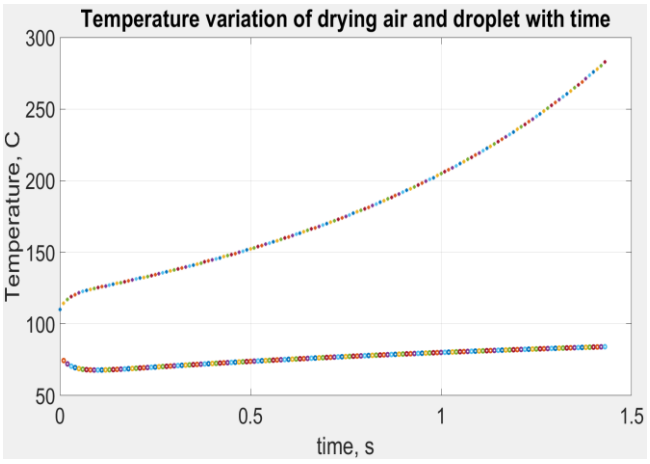

Figure 6. Temperature variation of drying air (top) and particle (d=400 μm). (Figure is in color in online version of paper).

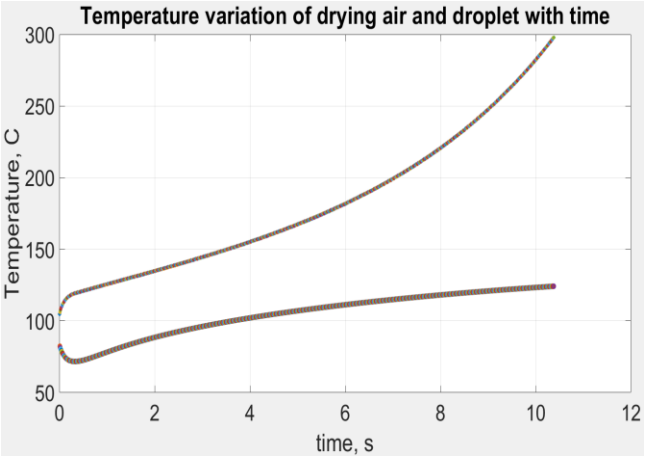

Figure 7. Temperature variation of drying air (top) and particle (d=1000 μm). (Figure is in color in online version of paper).

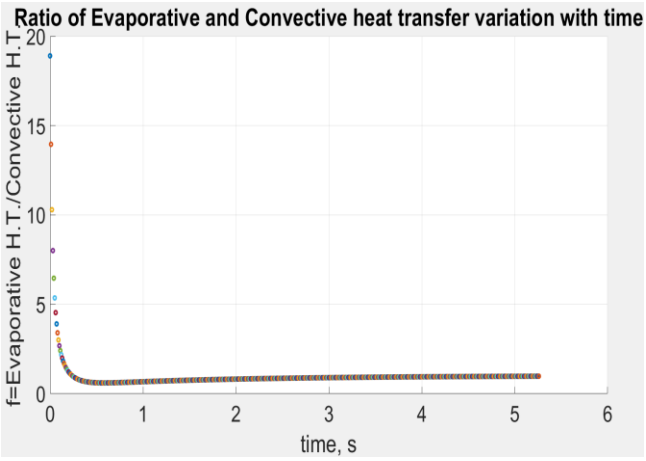

Figure 8. Ratio of evaporative heat transfer to convective heat transfer (d=750 μm). (Figure is in color in online version of paper).

In Figure 9, variation of Nusselt number variation is seen. The value of the Nusselt number decreases almost monotonically by 15%, due to the increasing dynamic viscosity of drying gas with temperature.

In Figure 10, variation of heat and mass transfer (*x1000*) coefficients are seen. While heat transfer coefficient increases with increasing time (or gas temperature), mass transfer coefficient remains relatively constant.

In Figure 11, evaporation rate variation in particles is seen. The initial very high water (humidity) concentration difference causes the mass transfer to be very high, however it falls very fast due to the particle's evaporative cooling, also causing its temperature to decrease. Later, with the increasing temperature difference between the particle and the drying gas, the drying process speeds up.

In Figure 12, variation of water mass fraction in particles is seen. As the particle loses water content by evaporation, the drying phenomenon accelerates due to the increasing temperature in drying gas as well as increasing concentration (humidity) difference between the particle surface and the gas.

In Figure 13, particle mass variation is seen. Its trend is very similar to Figure 12, as expected.

In Figure 14, absolute humidity variation (*W*) of drying gas is seen. Its trend is also similar to Figure 12.

In Figure 15, relative humidity variation (*RH*) of drying gas is seen. At the exhaust side it is around 12% while it is almost completely dry at the inlet.

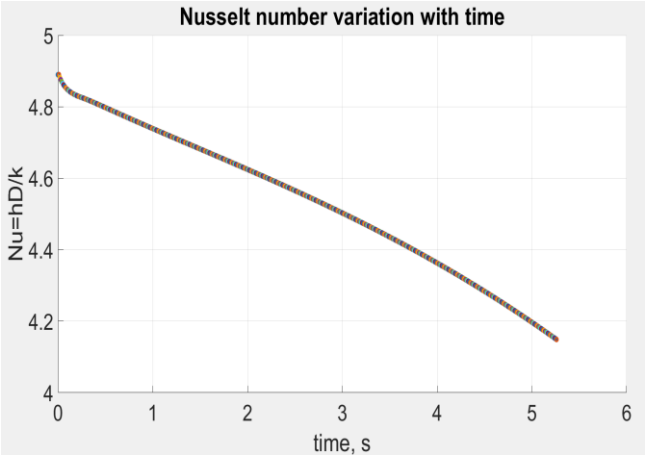

Figure 9. Nusselt number variation for particle (d=750 μm). (Figure is in color in online version of paper).

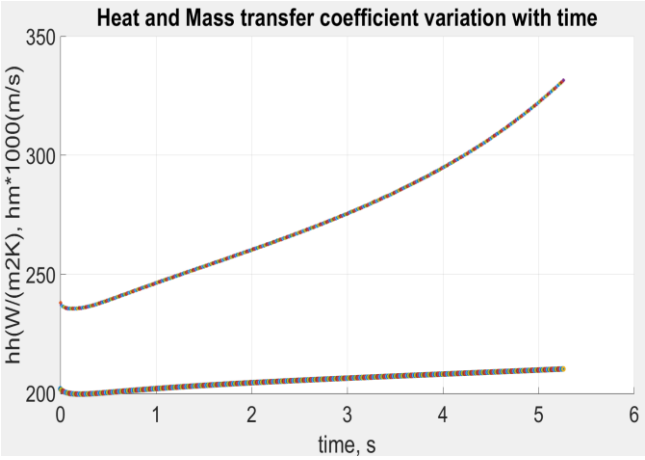

Figure 10. Comparison of heat (top) and mass transfer (x1000) coefficients (d=750 μm). (Figure is in color in online version of paper).

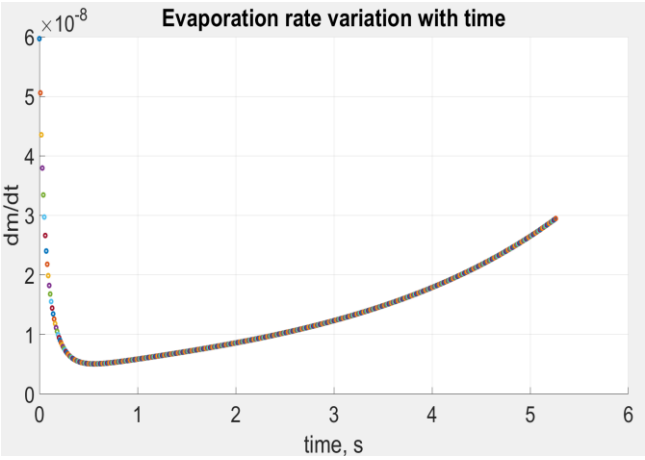

Figure 11. Evaporation rate variation for particle (d=750 μm). (Figure is in color in online version of paper).

The script was run for various final water contents of the final product to see the effect on the required drying time. It is observed that the drying time is inversely proportional to the final water content. The increase in drying time, or in other words energy consumption is about 3.3% when the final product water content is reduced from 3.6% to 2.4%.

Another interesting result obtained from a parametric study of the analytical model is the effect of the variation of excess air supply. When the air flowrate (stoichiometric + excess) is varied between 85%-105% of that of the problem at hand, the variation in the drying time is only within 0.4% of the 5.27 s obtained from the standard data. However variations in hot gas and final product temperatures are in the vicinity of 35ºC. Especially the final product temperature may be very critical as required by the subsequent processes.

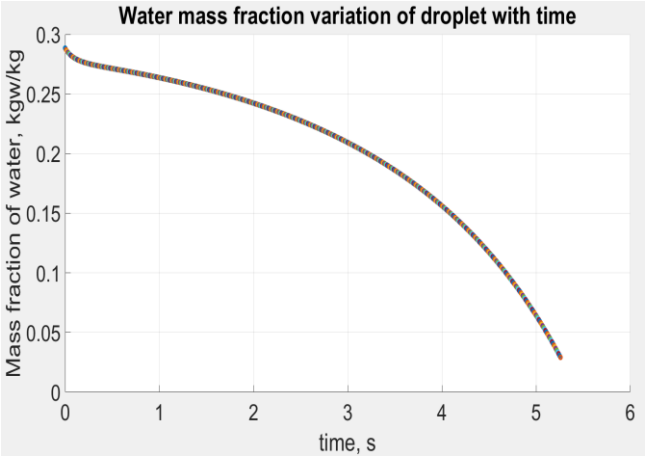

Figure 12. Water mass fraction variation in particle (d=750 μm). (Figure is in color in online version of paper).

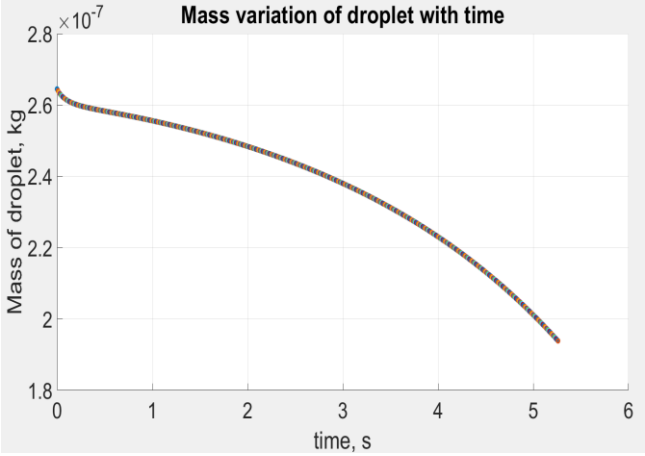

Figure 13. Mass variation in particle (d=750 μm). (Figure is in color in online version of paper).

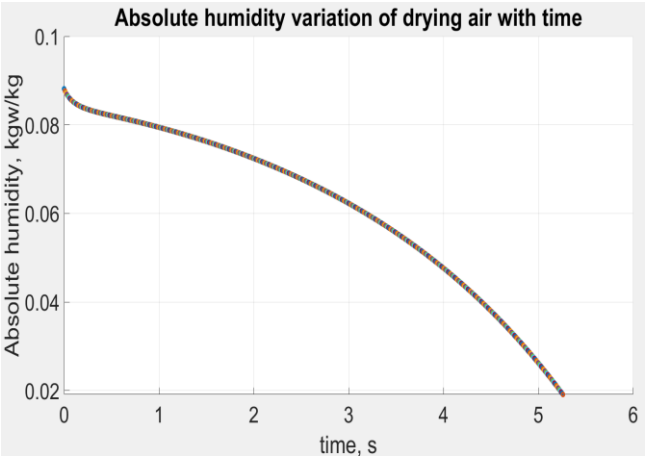

Figure 14. Absolute humidity variation in drying gas (d=750 μm). (Figure is in color in online version of paper).

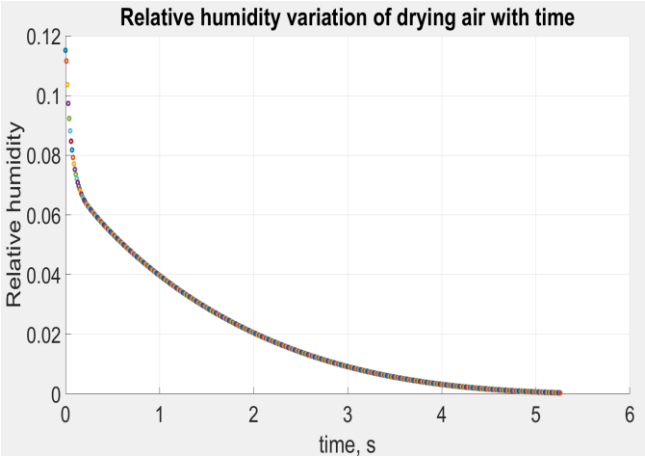

Figure 15. Relative humidity variation in drying gas (d=750 μm). (Figure is in color in online version of paper).

When the numerical results such as drying time, humidity and temperatures are compared to those provided by Ali [3], similar trends are observed. According to the researcher's plot for "residence time distribution of particles (Fig. 5.7)" provides a value about 5 s for a particle diameter of 750 μm which coincides with the required drying time.

4. Conclusion

In this study, spray drying of detergent particles of diameters *0.4-1 mm* by using counter-current air heated at around *300ºC* is investigated. Due to the complexity of the drying phenomenon, best operating parameters are usually difficult to determine resulting in poor quality of final product, being either too wet or over-dried and consumption of too much heating energy. The simulation results presented in this paper based on a mathematical model that takes into account many aspects of drying kinetics show that, by observing basic parameters, it is possible to fine tune the tower to optimum operating conditions which will not only increase the tower performance but decrease the energy consumption as well. It is recommended that the absolute humidity in tower exhaust be measured to be used as a control parameter for energy input.

Nomenclature

A	area [m^2]
c	specific heat [J/kg-C]
C	concentration []
d	particle diameter [μm]
D	tower diameter [m]
D_{AB}	mass diffusion coefficient [m^2/s]
$\vec{F}$	Force vector [N]
h	convective heat transfer coefficient [W/m^2C]
h_{mass}	convective mass transfer coefficient [W/m^2C]
H	tower height [m]
HHV	higher heating value [kJ]
i	enthalpy [kJ/kg]
L	latent heat [J/kg]
LHV	lower heating value [kJ]
m	mass [kg]
$\dot{m}$	mass flow rate [kg/s]
$\dot{n}$	discrete phase flow rate [particles/s]
Nu	Nusselt number [-]
$\dot{Q}$	heat transfer rate [W]
r	particle radius [m]
P	pressure [Pa]

Pr	Prandtl number [-]
Re	Reynolds number [-]
T	temperature [C]
$\vec{v}$	velocity vector [m/s]
V	scalar velocity [m/s]
$\dot{V}$	volumetric flow rate [m^3/s]
w	water content by weight [kg/kg or %]
W	absolute humidity [kg-w/kg-a]

Greek letters

α	thermal diffusivity [m^2/s]
μ	dynamic viscosity [Pa.s]
ρ	density [kg/m^3]

Subscripts

conv	convection
adia	adiabatic
b	buoyancy
diff	difference
d	drag
dry	dry (material)
exc	excess
exh	exhaust
fg	fluid-gas (in phase change)
g	gravitational
gas	gas
loss	loss
NG	natural gas
o	outer (surface)
p	particle
s	slurry
sto	stoichiometric
w	wet
wat	water
∞	far field

References:

[1] A. S. Mujumdar and V. Jog, "Simple Procedure for Design of a Spray Dryer," *Journal of the Institution of Engineers (India): Chemical Engineering Division*, vol. 57, pp. 134-138, Jun. 1977.

[2] P. Wawrzyniak, M. Podyma, I. Zbicinski, Z. Bartczak and J. Rabaeva, "Modeling of Air Flow in an Industrial Counter current Spray-Drying Tower," *Drying Technology*, vol. 30, no. 2, pp. 217-224, Nov. 2011, doi:10.1080/07373937.2011.618282.

[3] M. Ali, "Numerical Modeling of a Counter-Current Spray Drying Tower," Ph.D. dissertation, Ins. of Particle Sci. and Eng., School of Chemical and Process Eng., The Univ. of Leeds, Woodhouse, Leeds LS2 9JT, UK, 2014.

[4] E.A. Afolabi and K. R. Onifade, "Simulation of Air Residence Time Distributions of Spray Droplets in A Counter-Current Spray Dryer," *ARPN Journal of Engineering and Applied Sciences*, vol. 9, no. 2, pp. 145-152, Feb. 2014.

[5] M. Ali, T. Mahmud, P.J. Heggs, M. Ghadiri, A. Bayly, H. Ahmadian and L. M. de Juan, "CFD Simulation of a Counter-Current Spray Drying Tower with Stochastic Treatment of Particle-Wall Collision," *Procedia Engineering*, vol. 102, pp. 1284-1294, Jan. 2015, doi:10.1016/j.proeng.2015.01.259.

[6] M. J. Crosby, L. M. De Juan, E. Martin and G. Montague, "Particle size control of detergents in mixed flow spray dryers," *The Journal of Engineering*, vol. 2015, no. 3, pp. 102–107, Feb. 2015, doi:10.1049/joe.2014.0250.

[7] S. Gonzalez-Gallego, S. López and H. Alvarez, "A phenomenological-based model for a spray drying tower,"

Brazilian Journal of Chemical Engineering, Apr. 2023. [Online]. Available: https://link.springer.com/content/pdf/10.1007/s43153-023-00323-0.pdf

[8] B. Hernandez, B. Fraser, L.M. de Juan and M. Martin, "Computational Fluid Dynamics (CFD) Modeling of Swirling Flows in Industrial Counter-Current Spray-Drying Towers under Fouling Conditions," *Industrial & Engineering Chemistry Research*, vol. 57, pp. 11988-12002, Aug. 2018, doi:10.1021/acs.iecr.8b02202.

[9] Y. Xia, J. Lu, S. Jin and Q. Cheng, "Effect of pressure on heat and mass transfer performance in spray drying tower with low inlet temperature," *Applied Thermal Engineering*, vol. 218, pp. 1-15 Jan. 2023, doi:10.1016/j.applthermaleng.2022.119260.

[10] U. Jamil Ur Rahman, A.K. Pozarlik and G. Brem, "Experimental analysis of spray drying in a process intensified counter flow dryer," *Drying Technology*, vol. 40, no. 15, pp. 3128-3148, Dec. 2021, doi:10.1080/07373937.2021.2004160.

[11] A.M. Sefidan, M. Sellier, J.N. Hewett, A. Abdollahi and G.R. Willmott, "Numerical model to study the statistics of whole milk spray drying," *Powder Technology*, vol. 411, pp. 1-14, Oct. 2022, doi:10.1016/j.powtec.2022.117923.

[12] H. Jubaer, S. Afshar, J. Xiao, D.C. Xiao, C. Selomulya and M.W. Woo, "On the effect of turbulence models on CFD simulations of a counter-current spray drying process," *Chemical Engineering Research and Design*, vol. 141, pp. 592-607, Jan. 2019, doi:10.1016/j.cherd.2018.11.024.

[13] B. Hernandez, R. Mondragon, M.A. Pintoa, L. Hernandez, J. E. Julia, J.C. Jarque, S. Chiva and M. Martin, "Single droplet drying of detergents: Experimentation and modelling," *Particuology*, vol. 58, pp. 35-47, Oct. 2021, doi:10.1016/j.partic.2021.01.012.

[14] L. Chen, C. Chen, J. Yu and S. Jin, "Study on the heat and mass transfer characteristics of spray separation tower at low temperature and normal pressure," *International Journal of Heat and Mass Transfer*, vol. 153, pp. 1-17, Jun. 2020, doi:10.1016/j.ijheatmasstransfer.2020.119662.

[15] Y.A. Çengel and A.J. Ghajar, "Mass Transfer", in *Heat and Mass Transfer: Fundamentals & Applications*, 5th ed., New York, NY, USA: McGraw-Hill, 2015, ch. 14, sec. 1-6, pp. 835-854.

[16] M. Parti, "Mass Transfer Biot Numbers," *Periodica Polytechnica Ser. Mech. Eng.*, vol. 38, no. 2-3, pp. 109-122, Feb. 1994.

[17] W.W. Pulkrabek, "Thermochemistry of fuels" in *Engineering Fundamentals of the Internal Combustion Engine*, 2nd ed., Essex, UK: Pearson, 2014, ch. 4, sec. 1, pp. 153-155.

[18] F.C. McQuiston, J.D. Parker and J.D. Spitler, "Moist Air Properties and Conditioning Processes" in *Heating Ventilating and Air Conditioning – Analysis and Design*, 6th ed., Hoboken, NJ, USA: Wiley, 2005, ch. 3, sec. 2, pp. 51-53.

[19] S. Whitaker, "Forced convection heat transfer correlations for flow in pipes, past flat plates, single cylinders, single spheres, and for flow in packed beds and tube bundles," *AIChE Journal*, vol. 18, no. 2, pp. 361-371, Mar. 1972.